Stochastic Analysis of Crop Yield Uncertainty, Field Scale Study

Ayman Alzraiee and Luis García
Department of Civil and Environmental Engineering, Colorado State University

Abstract. Spatial heterogeneity of soil properties and uncertainty in root uptake model parameters make the numerical prediction of crop yield prone to a high degree of uncertainty. In this study, the spatial soil parameters are treated as multivariate correlated regionalized random parameters. Sequential indicator simulation is used to generate three-dimensional dependant realizations for hydraulic conductivity, porosity, Van Genuchten parameters and dispersivity. Other semi empirical parameters that control crop water uptake and subsurface drainage conductance where also randomized. Four hundred realizations for each of the soil parameters were generated and processed in the variably saturated flow and transport model (CSUID) to obtain the spatial statistical moments of the relative crop yield, root zone salinity and salt leaching fraction. The statistical distributions of drainage flow and salinity hydrographs were also calculated. Results show that parameter uncertainty significantly affects in-field relative crop yield variability and drainage flow and salinity effluent.

1. Introduction

As the demand on food, fiber and biofuel increases (Schnepf 2010), the burden on agricultural crop production is increasing. Several factors make such burden restrictive to the sustainability of crop production. Despite the increase in crop production induced by modern irrigation practices, the sustainability of this production is facing a real challenging situation because of the increase in root zone salinity worldwide. This occurs because of the accumulation of salts, brought by irrigation water, in the root zone. High salt concentrations in the root zone increase the osmosis pressure exerted by the plants to extract fresh water which could reduce crop yield if root zone salinity exceeds the salinity tolerance threshold for this crop (*Salinity Stress*).

Leaching the salts out of the root zone is commonly achieved by increasing the applied irrigation amount. However, this can have the side effect of developing a high water table (waterlogging) especially in cases where a shallow impermeable layer exists or when the storage capacity of the vadose zone is low. High seepage losses from nearby water bodies; such as streams, irrigation network and reservoirs, make the waterlogging problem not only a farm scale problem but a regional or basin scale problem. The long time saturation of the root zone reduces the crop yield by limiting the circulation of the air in the root zone causing reduction in the growth or irreversible damage to the crop (*Water Excess Stress*). In addition, shallow water tables usually aggravate the root zone salinity problem due to the saline water up flux. In these circumstances, a subsurface drainage system should be considered to control the water table while removing excess salts from the soil water system.

The combined effect of a shallow water table and high salinity is widely recognized as a plaque that impacts crop production worldwide. According to several

resources (Tanji 1990; Postel 1989; Umali and Umali-Deininger 1993; Ghassemi, Jakeman, and Nix 1995; and Wichelns 1999) lands affected by salinity comprise up to 28% of the irrigated land in the US, 23% in China and 21% in Pakistan. Worldwide economical losses are estimated by Ghassemi, Jakeman, and Nix (1995) to be around 11 billion dollars annually. This number is expected to be higher today.

Devising efficient irrigation and drainage management plans is one method to counterpart the current deterioration in land productivity or to reclaim existing saline land. The performance of any management plan could be evaluated based on, among other factors; the expected improvement in the crop yield, the extent of potential environmental risks that could result from drain effluent; and the long term performance of field productivity (sustainability of the cultivation activities, prevention of salt accumulation in the root zone). However, such evaluations could not be achieved at a reasonable cost without the use of numerical models that approximate the complex interactions between soil, water, plants and the atmosphere.

Despite the importance of numerical models, the validity of their predictions is still a matter of discussions among modelers (Konikow and Bredehoeft 1992; Oreskes, Shrader-Frechette, and Belitz 1994). Even calibrating the models using historical data of the system's response is not enough to guarantee the model validity because of the non-uniqueness of the calibrated model parameters. It seems that one unique and trusted prediction of numerical modes is far from being attained and it's more reasonable to deal with the problem of prediction using numerical models in a probabilistic framework. In this framework, model inputs are described by using probability distribution functions to reflect our lack of information. In other words, the uncertainty in the input parameters is propagated and its impact on output is statistically evaluated.

This study is part of a wider effort to study the problem of salinization and waterlogging in the Lower Arkansas River Basin in Colorado (Gates, et al. 2006). The Arkansas River is the highest impacted river by salinity in the US (Miles 1977; Tanji 1990). An extensive data sampling effort has been carried out from 1999 - 2009 to characterize the spatial and temporal extent of the soil salinization and waterlogging problem. Burkhalter and others (2005) developed a regional numerical model to investigate several management scenarios. Houk and others (2004) estimated the direct average forgone profit to be around $4.3 million/year in Otero County ($68/acre per year). The additional indirect and induced costs associated with waterlogging and soil salinization are estimated to increase by approximately 20% within this County.

In this study, the uncertainty aspect of the waterlogging and salinization problem is tackled on a field scale. Understanding the role that spatial variability plays in crop yield prediction is vital to guide future data collection efforts and to avoid risks that arise from the incomplete knowledge of the controlling parameters. In this research a multivariate Monte Carlo Analysis was used for a wide array of independent and dependant parameters that control crop yield and subsurface drainage performance on a farm. The controlling parameters are either spatially random correlated soil properties such as hydraulic conductivity, Van Genuchten parameters, dispersivity and porosity; or semi empirical parameters that control root growth, water uptake and drainage outflow calculation. The saturated and unsaturated flow and transport in a three dimensional field scale problem is

numerically simulated and the input parameters of the soil properties are randomized based on Sequential Indicator simulation.

The spatial variability of crop yield has been studied by a number of researchers. For example, Warrick and Gardner (1983) studied the impact of soil heterogeneity, represented as field capacity, wilting point and irrigation uniformity on crop yield. A linear response function between crop yield and soil and uniformity variability was assumed. Bresler and Dagan (1988) studied the impact of uncertainty of soil parameters and uptake model parameters for a one-dimensional model on yield uncertainty. The parameters are assumed statistically independent and uniform in the vertical direction. Rubin and Or (1993) used a stochastic analytic perturbation method to study the impact of soil spatial variability on water uptake by plants using a one dimensional steady state unsaturated flow. Muralidharan and Knapp (2009) showed that the variability of spatial infiltration increases the applied irrigation water and deep percolation flows by very substantial amounts compared to uniform infiltration. Montazar (2010) studied the impact of irrigation spatial uniformity on the yield of alfalfa hay.

Using numerical models to analyze the uncertainty associated with subsurface drainage systems is the subject of several studies. For example, Haan and Skaggs (2003) studied the impact of input parameter uncertainty on the drain out flow and crop relative yield using DRAINMOD. Monte Carlo simulations and first order approximation methods were used to determine the most sensitive uncertain parameter for a simplified layered system. Wang and others (2006) employed the generalized likelihood uncertainty (GLUE) estimation procedure to evaluate the uncertainty in DRAINMOD predictions of the subsurface drain flow. To the best of the authors knowledge, simulating the performance of subsurface drainage systems in a fully three dimensional heterogeneous aquifer system is absent from the published literature.

This study presents a comprehensive approach to deal with crop production uncertainty on a field scale. The paper includes 1) the temporally and spatially variability of the statistical moments of water content, salinity, root zone intake and water table depths using a probabilistic framework, 2) the spatial variability of crop yield statistical moments, 3) the performance of subsurface drainage in a three dimensional model with random soil properties, 4) the environmental risk of the drainage effluent in terms of the statistical moments of effluent volumes and its salinity.

2. Theoretical Framework

Crop yield is affected by a large number of parameters such as fertility, pests, soil chemistry, crop type, climate and cultivation practices among others. In this study, it is assumed that the agronomic conditions are excellent and the only limiting factors are the soil hydrosalinity conditions. The crop yield can be modeled using equation (1) which is based on the assumption of a linear relationship between the relative evapotranspiration and relative yield.

$$\frac{\boldsymbol{Y_a}}{\boldsymbol{Y_m}} = \mathbf{1} - \boldsymbol{k_y}\left(\mathbf{1} - \frac{\boldsymbol{ET_a}}{\boldsymbol{ET_m}}\right) \tag{1}$$

Where Y_a is the actual dry matter yield [M], Y_m is the maximum harvested dry matter yield [M], k_y is the yield response factor, ET_a is the total (seasonal) actual evapotranpiration, and ET_m is the maximum seasonal evapotranpiration which can be obtained from climatic data.

According to equation (1), the calculation of relative crop yield is equivalent to the calculation of actual ET. The total actual evapotranspiration ET_a is approximated by integrating the temporal extraction rate over the growing season and over the root zone depth (see equation (2)).

$$\boldsymbol{ET_a = \int_0^T \int_0^{D(t)} Q_r(z,t)\, dzdt} \tag{2}$$

Where $Q_r(z,t)$ is the temporal root extraction [L^3/T] at a vertical depth z per unit soil volume, T is the overall season period [T], D is the root depth [L]at time t.

It's appropriate in this study to adopt the macroscopic modeling of the root uptake in which the uptake is represented as a nonlinear sink term in the flow and transport equation. The nonlinearity of calculating the root uptake $Q_r(z,t)$ stems from its dependency on the water matric head and the osmotic head induced by salinity. For overviews of root uptake models readers are referred to Molz (1981) and Hopmans and Bristow (2002). The overall sink term that accounts for root density and geometry, water matric and osmotic pressure and root growth stage are summarized in equation (3).

$$\boldsymbol{Q_r(z,t) = \lambda(z,t).\frac{ET(t)}{\Delta A}.\alpha(\psi,\psi_o).C_o} \tag{3}$$

Where $ET(t)\ is$ the reference evaporation [L/T], C_o is the crop growth coefficient at time t, $\boldsymbol{\Delta A}$ is area L^2 and $\lambda(z,t)$ is the root density equation that describes the density and the geometry of the root network with respect to the depth and can be calculated using the S function equation (4).

$$\boldsymbol{\lambda(z,t) = \frac{-1.6z}{D(t)^2} + \frac{1.8}{D(t)}} \tag{4}$$

Where z is the depth at which the root density is calculated [L] and $D(t)$ is the root depth at current time [L]. The temporal root growth can be approximated using the Hank Hill Equation (5)

$$\boldsymbol{D(t) = \frac{D_{max}}{\left(1+\exp\left(a-b\frac{t}{t'}\right)\right)}} \tag{5}$$

Where $D(t)$ is the root depth at time t, D_{max} is the maximum root depth, t' is the end of the crop's growth third stage, and a, b are empirical coefficients.

Feddes et al. (1976) pioneered describing the sink term as a function of the water content and Van Genuchten and Laboratory (1987) extended it to incorporate osmosis head. In this paper, we modify Cardon and Letey (1992a) equation, which is a slight modification of Van Genuchten and Laboratory (1987), to account for waterlogging.

Equation (6) is the final equation that accounts for water deficit stress, salinity stress and water excess stress (waterlogging).

$$\boldsymbol{\alpha(\psi,\psi_o)} = \begin{cases} \dfrac{\mathbf{1}}{\mathbf{1}+\left(\dfrac{\boldsymbol{\psi}}{\boldsymbol{\psi_{50}}}+\dfrac{\boldsymbol{\psi_o}}{\boldsymbol{\psi_{o50}}}\right)^{\boldsymbol{P}}} & \boldsymbol{\psi(z,t) < \psi_s} \qquad (\mathbf{6.a}) \\ \dfrac{\left(\dfrac{\boldsymbol{\psi}}{\boldsymbol{\psi_s}}\right)}{\mathbf{1}+\left(\dfrac{\boldsymbol{\psi}}{\boldsymbol{\psi_{50}}}+\dfrac{\boldsymbol{\psi_o}}{\boldsymbol{\psi_{o50}}}\right)^{\boldsymbol{P}}} & \boldsymbol{(z,t) \geq \psi_s > 0} \qquad (\mathbf{6.b}) \end{cases}$$

Where p is a parameter close to 3, ψ_{50} is the capillary head at which the root uptake is reduced by 50% and $\psi_o = 0$ [L], is the osmotic head at which root uptake is reduced by 50% and $\psi = 0$[L], $\psi(z,t)$ [L]is the capillary head [L] and $\psi_o(z,t)$ is the osmotic head [L], ψ_s is the head threshold after which oxygen deficiency starts to occur[L]. It is recognized that the water excess stress (near saturation cases) does not impact the root uptake instantaneously (Feddes et al. 1976) but could take the crop a few days (for example, 2 days) to impact the root uptake. As a result, Equation 6.b will not be active until the matric head is equal or above ψ_s for a period of two days.

The evaluation of equation (6), the capillary head and the salinity are required to be calculated. The continuity equation for flow and transport of water and salts in a variably saturated aquifer are mathematically modeled using two partial differential equations for flow and transport (equations 7 and 8).

$$\frac{\partial}{\partial x_i}\left(\boldsymbol{K_i(\psi)}\frac{\partial \boldsymbol{h}}{\partial \boldsymbol{x_i}}\right) + \boldsymbol{Q_s} = \left(\frac{\boldsymbol{\theta}}{\boldsymbol{\theta_s}}\boldsymbol{S_s} + \boldsymbol{C(\psi)}\right)\frac{\partial \boldsymbol{h}}{\partial \boldsymbol{t}} \tag{7}$$

$$\frac{\partial}{\partial x_i}\left(\boldsymbol{\theta D_{ij}}\frac{\partial \boldsymbol{C}}{\partial \boldsymbol{x_j}}\right) - \frac{\partial}{\partial \boldsymbol{x_i}}(\boldsymbol{\theta v_i C}) + \boldsymbol{Q_s C_s} = \frac{\partial(\boldsymbol{\theta C})}{\partial \boldsymbol{t}} \tag{8}$$

Where $K_i(\psi)$ is the hydraulic conductivity [L/T], ψ is the capillary head [L], h is the total head [L] ($\psi = h - z$), Q_s is the sink or source term per unit volume [T^{-1}], θ is the moisture content [L^3/L^3], θ_s is the soil porosity [L^3/L^3], S_s is the specific storage [L^{-1}], $C(\psi)$ is the specific capacity [L^{-1}], x is a space vector [L] and $i = 1,2,3$ represents three-dimension space, t is time [T]. D_{ij} is the hydrodynamic dispersion [L/T2], C is the salinity concentration [M/L3], v_i is the seepage velocity [L/T].

The sink term Q_s is the net sinks/sources term [T^{-1}]. Q_i is the irrigation rate [L^3T^{-1}] which is a model input parameter, Q_d is the drain outflow, Q_r is the root uptake [L^3T^{-1}] calculated from equation (3).

$$Q_s = \frac{(Q_r + Q_i + Q_d)}{\Delta V} \tag{9}$$

It can be noted that, Q_r is the head and concentration dependant sink term while the Q_d is the head dependant sink term and is calculated using equation (10) (Harbaugh et al. 2000)

$$Q_d = C_d(h - Z_d) \tag{10}$$

Where $Q_d\ is$ the drain outflow [L^3/T], C_d is the conductance [L^2/T], h is the hydraulic head [L] at the drain pipe and Z_d is the drain elevation [L].

Solving equations 7 and 8 requires knowledge of the relationship between moisture content and capillary head that are modeled via the Van Genuchten (1980) model,

$$\boldsymbol{\theta(\psi) = \theta_r + \frac{\theta_s - \theta_r}{(1+(\alpha|\psi|)^{\beta})^{1-\frac{1}{\beta}}}} \tag{11}$$

Where θ_r is the residential moisture content [L^3/L^3], α is a fitting parameter related to the inverse of the air entry suction, $\alpha > 0$ [L^{-1}], β is a measure of the pore size distribution, $\beta > 1$.

3. Stochastic Analysis

The uncertainty in the predictions made by the set of deterministic equations in the preceding section stems, to a large extent, from the parameters uncertainty. Some of these parameter uncertainty results from its unknown spatial structure, namely hydraulic conductivity, specific storativity, porosity, dispersivity, and Van Genuchten parameters. Treating these parameters within the context of random spatial functions is the basis for multivariate Monte Carlo analysis presented in the next section.

3.1 Joint Simulation of Several Variables

Generally speaking, consider N regionalized soil properties $Z_1, Z_2, \dots Z_N$. Each of them has a number of field measurements $D_1, D_2, \dots D_N$ respectively. The *N* soil properties are normally distributed, or can be transformed to be normal and correlated. The normality assumption can be relaxed as shown later. Given the previous considerations, the objective of the geostatistical simulation is to generate N dependant realizations for each soil property.

The Sequential Indicator Simulations (SIS) method (Deutsch and Journel 1997) is employed in this paper due to its flexibility in incorporating hard and soft information about simulated parameters. The SIS method aims at calculating a least-squares estimate of the conditional cumulative function $F(Z_{i,k})$ at a pre specified cutoff $Z_{i,k}$, where i is the soil property index and k is the cutoff index. Usually 4 to 10 cutoff values are used to approximate the cumulative distribution function $F(Z_i)$ (Deutsch 2002). In this paper the same number of cutoffs is used for all the soil variables ($Z_1, Z_2, \dots Z_N$). Moreover, the cutoff values are chosen in a consistent manner for all the variables, i.e. the k^{th} cutoff, for example, is calculated for any variable Z_i using equation (12)

$$\mathrm{Z_{i,k}} = \mathrm{Z_{o,k}}\sigma_{\mathrm{Z_i}} + \mu_{\mathrm{Z_i}} \tag{12}$$

Where $Z_{o,k}$ is an arbitrary cutoff value in the standard normal distribution ($\mu_o = 0, \sigma_0 = 1$), σ_{Z_i} and μ_{Z_i} are the standard deviation and the mean of the variable Z_i respectively. In other words, equation (12) calculates cutoff values for each of the soil variables at the same standardized CDF cutoff $Z_{o,k}$.

Without losing generality, the sequential simulations of the variables can be started at parameter Z_1. The CDF value $F(Z_{1,k}(x))$ at the k[th] cutoff and at x spatial position should be 0 or 1, at locations where Z_1data are available, according to equation (13).

$$\mathrm{F(Z_{1,k}(x))} = \begin{cases} 1 & \mathrm{Z_1(x) < Z_{1,K}} \\ 0 & \text{otherwise} \end{cases} \tag{13}$$

Where x is the spatial position of the field measurement. For any other location x' where no field measurements are available, $F(Z_{1,k}(x'))$ can be estimated using equation (14) (Deutsch and Journel 1997).

$$F\left(Z_{1,k}(x')\right) = \sum_{x=1}^{n} \lambda_x . F\left(Z_{1,k}(x)\right) + [1 - \sum_{x=1}^{n} \lambda_x] F(Z_{1,k}) \tag{14}$$

where $F(Z_{1,k})$ is the global CDF based on the data D_1, n is the number of field measurements and λ_x are the simple kriging weights that can be calculated from a set of linear equations as in equation (15).

$$\sum_{y=1}^{n} \lambda_y \, C_I^{Z_{1,k}}(y - x) = C_I^{Z_{1,k}}(x' - x), \quad x = 1, .. n \tag{15}$$

where $C_I^{Z_{1,k}}(x' - x)$ is the indicator covariance of variable Z_1at the k cutoff.

Hence Z_1 is normally distributed, or transformed to be normal, and correlated with the remaining $Z_2, .. Z_N$, therefore the conditional CDF given the data $Z_2, .. Z_N$ is normally distributed and can be exhaustively described by its conditional mean and conditional variance as expressed in equations (16) and (17).

$$\boldsymbol{m(Z_1(x)|D_2, \ldots D_N) = m(Z_1(x)|D_2, .. D_{N-1}) + \rho_{1,N-1}\left(\frac{\sigma(Z_1(x)|D_2, .. D_N)}{\sigma(Z_{N-1})}\right)(Z_{N-1} - m(Z_{N-1}))} \tag{16}$$

$$\boldsymbol{\sigma(Z_1(x)|D_2, \ldots D_N) = \sigma(Z_1(x)|D_2, \ldots D_{N-1})\left(1 - \rho_{1,N-1}\right)^{0.5}} \tag{17}$$

This attractive property of a normal distribution is the motivation behind transforming the soil property using the Johnson transformations family (Johnson et al. 1995). However, it's possible that none of the distributions in the Johnson family produces a normally distributed variable. In such situation, the conditional CDF can be non-parametrically inferred by slicing the scatter plot of two correlated parameters at known parameter values. In this paper the soil parameters were transformed and the transformation that produced the lowest Chi-squared Goodness of Fit Test statistic is used. Consequently, knowing the conditional mean and standard deviation of the normal distributed Z_1variable at location x'

is all what is needed to determine the $F\left(Z_{1,k}(x')|D_2, \ldots D_N\right)$. The same procedures should be repeated at all cutoffs. In SIS simulations one Z_1 value is randomly sampled from the calculated CDF at x' location.

In conclusion, the simulation is repeated at all cell nodes to produce a three dimensional realization of the variable Z_1. Recall that every new simulated CDF should be conditioned on previously simulated values as well as the hard data. The resulting realization can be expressed mathematically using equation (18).

$$l_{Z_1}: \{(Z_1(x)|D_1, .. D_N), x \in A\} \tag{18}$$

Given the simulated soil property realization l_{Z_1}, it's required to continue the simulation to the next soil property Z_2. The same steps can be followed however this time the simulation of $Z_2$is conditioned on the hard data $(D_1, .. D_N)$ and the previously simulated Z_1. To generalize the procedures, variable Z_i can be simulated by conditioning the simulation on all previously simulated variables $Z_1, \ldots Z_{i-1}$ and hard data $D_i, .. D_N$ as shown in equation (19).

$$l_{Z_i}: \{(Z_i(x)|(Z_1, .. Z_{i-1}, D_i, .. D_N), x \in A\} \tag{19}$$

In this paper, the order of the variables simulated is set by simulating the parameter that has the largest number of field measurements, namely the hydraulic conductivity, followed by the parameter that is highly correlated with the conductivity which is the pore scale parameter and so on.

3.2 Covariance Inference

Solving equation (15) requires the knowledge of the covariance model at the k^{th} cutoff and also requires that the transformed variables using equation (13) are stationary at the k^{th} cutoff. Under the stationary assumption the variogram and covariance models are equivalent, namely $\gamma(h) = C(0) - C(h)$. Given that the number of cutoffs is $\boldsymbol{K}$, then KN covariance models are required. Inference of the variograms for all variables requires a large number of field measurements that are usually not easy to obtain. However, it is possible, assuming the validity of the intrinsic coregionalization model (Wackernagel 2003), to make use of the abundant data for a certain variable to infer the variograms for other variables. For example, the abundant data for hydraulic conductivity can be used to infer the variogram for Van Genuchten parameters and porosity. The validity of intrinsic coregionalization models is possible if the multivariate correlation structure of a set of variables is independent of the spatial correlation. This model bases on a Markov screening hypothesis, in which a co-located primary data screens the influence of a distant data values on the secondary variable (Journel 1999). As a result, the covariance model for any variable Z_i can be obtained from equation (20)

$$C_{Z_i}(h) = \sigma_{Z_i}\rho(h) \tag{20}$$

Where $\rho(h)$ is the correlogram that is inferred from another variable Z_j that has abundant field measurements.

$$\rho(h) = \frac{C_{Z_j}(h)}{{\sigma_{Z_j}}^2} \tag{21}$$

Therefore equation (21) reveals that all variables have the same spatial correlation scale but the sill value is scaled by the variance of the variable.

4. Site Description

The site of this study, known as field 17, is located in the neighborhood of the town of Rocky Ford, Colorado. The groundwater flow regime direction is from the southwest to the northeast and the water table depths range between 0.6 m in the southwest to 2.4 m in the northeast. The groundwater salinity in field 17 was found to range between 1.33 – 2.49 ds/m (843 mg/l – 1,566 mg/l). The average groundwater salinity was 2ds/m (1,280 mg/l) and the standard deviation was 0.44 ds/m. According to FAO report 48 (Rhoades et al. 1992), this level of salinity is classified as slight to moderate salinity. The soil type in the region is alluvial deposits that consist of a silty loam clay layer in the upper surface and loam to sandy loam substrata (USDA, 1971a; USDA, 1971b). The water table and groundwater salinity were monitored using 33 observation wells. Part of the field was chosen for the numerical simulation which is the part that has high water table and high soil salinity. A subsurface set of drainage pipes is intended to be installed to alleviate the water logging and salinity problems.

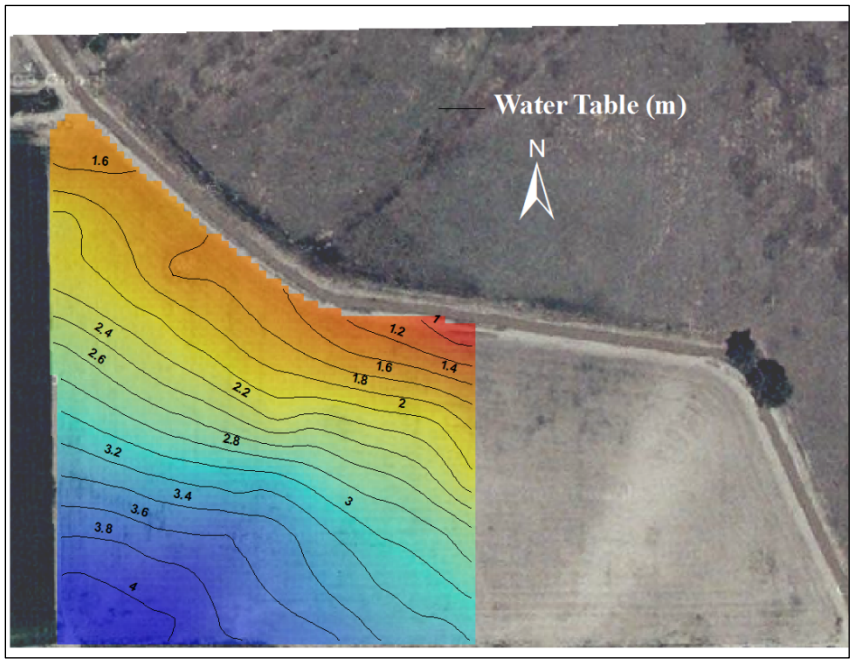

Figure 1. Site Map and the Numerical Domain

5. Parameter Statistical Distributions

The uncertainty in the prediction of crop yield, drain outflow and salinity calculated from equations (1) to (11) is controlled by 18 uncertain parameters. These parameters are grouped in three categories, 1) three dimensional soil properties, which are the hydraulic

conductivity K; the porosity θ_s; the Van Genuchten parameters θ_r, α, β; soil specific storativity S and dispersivity α_z; 2) two dimensional parameters such as irrigation weight w_i (irrigation uniformity) and preferential flow fraction p_i which is the fraction of irrigation water that reaches the water table instantaneously; and 3) semi empirical parameters that control yield, water uptake and drainage flow which are the yield response factor K_y, uptake model parameters ψ_{50}, ψ_{o50}, ψ_s, P; root growth rate parameters a, b; crop growth parameter C_o and drain conductance coefficient C_d. Most of these parameters are randomized as shown in the following sections.

5.1 Three dimensional Soil Spatial Parameters

All the three dimensional soil parameters are randomized except for the specific storativity. Since the specific storativity is a function of the water compressibility and soil matrix compressibility, it has a small impact especially in shallow unconfined aquifers such as the field under study. The multivariate Sequential Indicator Simulation, outlined in section (3), is employed to generate equally probable three dimensional simulations for (K, θ_s, θ_r, α, β) while dispersivity is estimated based on a regression model as will be shown later in this paper. The Cone Penetration Test (CPT) is used to estimate the hydraulic conductivity vertical profiles at 15 positions in field 17 with vertical depths ranging between 6m to 20m. The resulting measurements are averaged at 10cm vertical intervals resulting in 665 hydraulic conductivity measurements. A number of core samples (37 cores) were used to obtain the Van Genuchten parameters and porosity. Only eight of these core samples have also hydraulic conductivity values. Obviously, these eight samples are not enough to calculate the correlation between the hydraulic conductivity and the Van Genuchten parameters. Therefore, a soil database (ROSSETA database) for the five parameters (K, θ_s, θ_r, α, β) (Schaap, Leij et al. 2001) which include 650 records are used for two purposes, first, to estimate a better correlation coefficients among the five parameters and, second to select a suitable normal transformation scheme. Johnson transformations family is used to transform the parameters and the scheme that achieves the lower Chi-squared Goodness of Fit Test statistic is used (Table 1).

The transformed field measurements are simulated using the multivariate SIS using five cutoff values (Table 3). The transformed hydraulic conductivity field measurements are used to calculate the experimental indicator horizontal and vertical variograms at each of the five cutoffs. Thus, ten experimental variograms were obtained and the spherical variogram functions were fitted. A summary of the variogram fittings is shown in Table (4). Recall that according to the intrinsic coregionalization model adopted in section (3.2) the correlation scales of the hydraulic conductivity indicator variograms are the same for θ_s, θ_r, α and β. The Geostatistical Library (GSLIB) (Deutsch and Journel 1997) Sequential Indicator Simulation method is used successively to simulate the parameters in the following order: K, $\beta, \theta_s, \theta_r, \alpha$.

Table 1. Choosing the Best Normal Transformation Scheme

Parameter	Mean	Variance	Chistat
thetaR	0.11	0.002	97.36
thetaS	0.41	0.01	175.27
alpha	0.05	0.006	65.95
n	2.08	1.12	320.02
log(thetaR)	-1.02	0.07	11.33
log(thetaS)	-0.39	0.01	95.82
log(alpha)	-1.34	0.02	33.12
log(n)	0.27	0.04	482.12
SB(thetaR)	-0.47	0.29	11.69
SB(thetaS)	-0.35	0.2	74.35
SB(alpha)	-0.36	0.15	107.75
SB(n)	-0.79	0.67	55.27
SU(thetaR)	-1.65	0.35	11.33
SU(thetaS)	-0.22	0.03	95.82
SU(alpha)	-2.4	0.11	33.12
SU(n)	1.31	0.2	482.12

Table 2. Statistical Properties of Transformed Data

	Mean	STD	Transformation	LN(K)	θs	θr	α	β
LN(K)	-0.574	1.788	Log10	1.00	-0.19	-0.42	-0.26	0.77
θs	0.451	0.047	SB	-0.19	1.00	0.59	0.60	-0.36
θr	0.160	0.050	Log10	-0.42	0.59	1.00	0.55	-0.29
α	0.046	0.030	Log10	-0.26	0.60	0.55	1.00	-0.47
β	1.529	0.329	SB	0.77	-0.36	-0.29	-0.47	1.00

Lognormal $LN: Y = \ln(x)$

Log Ratio $SB: Y = \ln\left(\frac{X-A}{B-X}\right)$

Hyperbolic Arcsine $SU: Y = sinh^{-1}(x) = \ln\left[x + (1+x^2)^{0.5}\right.$

Table 3. Cutoff Values of the Transformed Parameters

Soil Property Cutoff	θr	Θs	α	β	K
C1	-1.00	-2.09	-1.64	-2.39	-3.01
C2	-0.93	-1.35	-1.51	-1.39	-2.00
C3	-0.80	0.11	-1.26	0.58	0.00
C4	-0.73	0.84	-1.13	1.57	0.99
C5	-0.67	1.57	-1.00	2.55	1.99

Table 4. Indicator Variogram Parameters

Normalized Cutoff Value (Z)	-1.37	0.8	0.32	0.88	1.44
Vertical Correlation Scale (m)	1.1	1.3	1.4	1.5	1.5
Horizontal Correlation Scale (m)	126	117	153	72	75
Sill Value	0.2	0.23	0.3	0.11	0.03

5.2 Hydrodynamic Dispersivity (α_x)

It is expensive and time consuming to obtain site-specific dispersivity values (for example, tracer test); on the other hand laboratory column tests usually reflect scales that are much smaller than site scales. This is beside the scale dependency of the dispersivity. Other methods are correlation methods (Xu and Eckstein 1997) that use correlation between dispersivity and other easy to obtain soil properties. In this research a simple correlation method form (Xu and Eckstein 1997) was chosen. It was found that the correlation between α_x and the reciprocal of porosity is 0.84 and the following model can describe this relationship with an R^2 of 0.74.

$$\alpha = -25.47 + 12.40\left(\frac{1}{\theta_s}\right) \tag{22}$$

Unfortunately, the limitation of this regression model is the inability to deal with porosity values greater than (0.486) due to resulting in negative dispersivity. To circumvent this problem, the previous model was retrofitted to a polynomial function that has its root at $\theta_s = 0.668$, which is a very rare event. Both models have almost the same performance for $\theta_s < 0.486$.

$$\alpha_z = -1268.9\theta_s^3 + 1950.6\theta_s^2 - 990.64\theta_s + 169.72 \quad (23)$$

Where α_z is the dispersivity value in (mm). Equation (23) enables us to calculate the vertical dispersivity at each cell using the porosity field.

5.3 Irrigation spatial depth and Uniformity

The uniformity of spatial depth is significantly impacted by the irrigation system used. For example, the sprinkler system usually has high uniformity coefficients, for example Christiansen's Coefficient (CU) that is mainly impacted by the wind speed and direction. Other factors that affect the CU for sprinklers are the layout and spraying hydraulics. In surface irrigation systems, the topography, bed geometry, vegetation density and soil properties impact the uniformity of the irrigation. In this study a sprinkler system is assumed to be used. The CU values of less than 84% are considered low according to Bliesner and Keller (2001). Assuming a unity irrigation depth (called *'irrigation weight'*), it's reasonable to statistically model this property using a normal distribution $N\sim(\mu = 1, \sigma_w^2)$. According to Montazar (2010), the normal distribution is a good model for the case of sprinkler systems but might not be proper for surface or drip irrigation systems due to the role of land topography affecting surface irrigation and due to the design and the hydraulics of drip irrigation systems.

The actual irrigation depth can be calculated by multiplying the average irrigation depth by the irrigation weight. The aim of this research is to select a value of σ_w^2 based on the uniformity coefficient. First, it is needed to randomly select a Christiansen's Coefficient CU from the arbitrarily selected uniform distribution $U\sim(a = 95\%, b = 85\%)$. Next using the sampled CU, the irrigation depths variance can be computed from equation (24).

$$\sigma_w^2 = \frac{\pi}{2}\left(1 - \frac{CU}{100}\right)^2 \quad (24)$$

The previous equation is derived by substituting the mean absolute deviation, in the CU equation (Hoffman et al. 2007), by the irrigation depth variance.

5.4 Preferential flow

The flow and transport in porous media can be either rapid macro pores flow and transport (direct drainage) or matrix slow flow (general drainage) (Steenhuis et al. 1994). The spatial distribution of shrinking cracks or bio-holes is complex and unpredictable. A simplified method is adopted to quantify the fraction of irrigation or rainfall water that rapidly reaches the water table. To the extent of the authors knowledge there is no published data that quantifies the amount of surface water that rapidly reaches the groundwater table. As an alternative, it is assumed that the bypass flow fraction is a spatially random, uniformly distributed and spatially independent regionalized variable. The uniform distribution of the bypass adopted is $\mathrm{U}\sim(\mathrm{a} = 0, \mathrm{b} = 10\%)$. This distribution reflects a high degree of uncertainty regarding bypass flow.

5.5 Root Uptake Model Parameters

Equation (6) describes the root uptake model where four semi empirical parameters are required to predict the root extraction ($\psi_s, \psi_{50}, \psi_{o50}, p$). The parameter ψ_s represents the metric head value at which the yield will decrease due to oxygen deficiency. Veenhof and McBride (1994) suggested values for ψ_s to be between -1cm to -30cm. In line with these findings, a uniform distribution is used U~(a $= -1$, b $= -30$)cm. Cardon and Letey (1992) used a value of $\psi_{o50} = -4300$ cm and they estimated ψ_{50} to be within the range of $-2500\ to\ -6500$ cm. Shalhevet and others (1986) used $\psi_{o50} = -6400cm$ for alfalfa. In this paper, dry biomass data for alfalfa that were collected from field 17 is used to calibrate the parameters in equation (6). Using $\psi_{o50} = -6400cm$ as in Vinten and Meiri (1986) the values of ψ_{50} are estimated at different metric heads. The value of ψ_{50} was plotted versus the summed square errors of yield estimation at different metric heads (Figure 2). From Figure 2 it can be seen that a reasonable distribution of ψ_{50} is U~(a $= -800$, $b\ -3000$) cm. The parameter $\boldsymbol{p}$ is dealt with as a deterministic value equal 3.

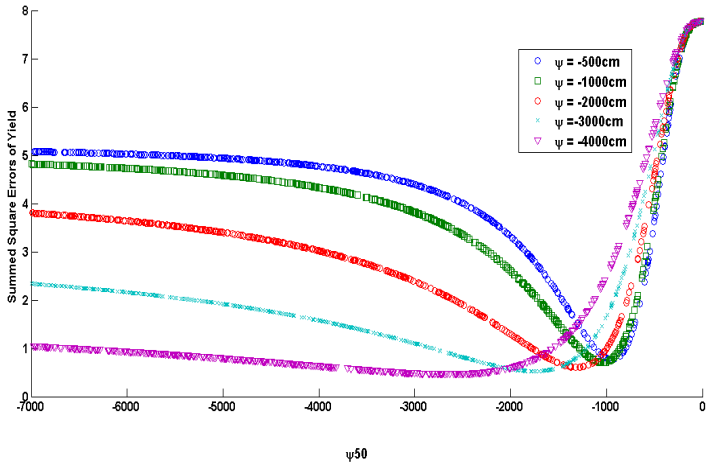

Figure 2. Estimating ψ_{50} values using dry alfalfa biomass data

5.6 Drain Conductance

The drain outflow in equation (10) is a head dependant flow. The conductance [L^2/T] quantifies the resistance that water flow experiences to enter the drain. Specifically, the value of conductance reflects entrance resistance and gravel envelop resistance. Usually the values of conductance are determined during model calibration procedures. Deverel and Fio (1991) used field data of head at the drain and outflows and calculated conductance values based on equation (10). The values obtained were within the range of 0.27 m^2/day/m to 0.44m^2/yr/m. Conductance values estimated by calibration by Goswami and Kalita (2009) are within the range of 0.15 and 0.58 m^2/day/m. In this study and in accordance with published conductance values, a wide uniform distribution is used $U\sim(a = 0.01, b = 2)$ m^2/day/m.

6. Numerical Simulation

The equations (1) to (11) are solved using the CSUID model (Alzraiee et al. 2009). This model is a three dimensional variably saturated flow and transport model in a heterogonous porous media. The resulting nonlinear finite difference equations of flow and transport are solved using the precondition conjugate gradient method (Harbaugh et al. 2000). The horizontal cell sizes used is 10m x 10m and the vertical cell size is 0.25m. The number of cells in the horizontal plane is 30 for the east-west direction and 38 cells in the north-south direction. Twenty layers, each 25cm, were used. The general boundary conditions are used to describe the boundary of the field. The upstream and downstream boundaries are each divided into 3 sections to represent the head variability in the boundary. The salinity of the lateral flux induced by the general boundary condition was chosen to be consistent with groundwater salinity measurement at these boundaries.

The simulation season period is 75 days. A root zone depth of 0.5 m is assumed and its growth rate is controlled by the Hanks Hill equation. The initial growth stage is 20 days, the development stage is 30 days, the middle stage is 15 days and the late stage is 10 days. The crop coefficients are 0.7, 1.0, and 0.95 for the initial, middle and late crop coefficients respectively. The developing stage crop coefficient is linearly interpolated between 0.7 and 1 and the late crop coefficient is a linear interpolation between 1 and 0.95. The reference evapotranspiration is assumed to be uniform in space and constant over the growing season (5mm). The salinity, as TDS, of the irrigation water is assumed to be 350 mg/L which is consistent with the salinity of the surface water in the valley.

The initial water table is dealt with as a deterministic kriged surface using 33 observation wells. The initial salinity concentration is obtained by kriging the salinity measurements and it is assumed that the vertical salinity profile is uniform due to the lack of information about the salinity stratification.

7. Results and Discussion

The hydrological responses of the aquifer systems, which include water table level, root zone salinity, relative crop yield and leaching fraction vary spatially and temporally. Due to the large numerical outputs, at each time step and each numerical node, the discussion of the results is limited to the end of the season.

Water Table

The spatial distribution of the first and the second statistical moments of the water depth at the end the growing season are shown in figures 5 and 6. Comparing the water depth before and after installing the drains shows that the average water table is reduced and the waterlogging problem in the southern west part of the field has disappeared. The average water table depths range between 1.07m and 2.36m. The standard deviation of the of water table depths range between 0.006m in the field downstream and 0.28m in the field upstream. It can be shown that the coefficient of variation is in the range of 0.003 to 0.14 which reflects a narrow range of variability. This is due, in part, to the impact of the drain which fixes the water table around its elevation.

Root Zone Salinity

The average root zone salinity values range between 350mg/L and 1,307mg/L. High salinity averages occur mainly in the upstream of the drain pipes where the water table is relatively high (shallow). Salinities before the installation of the drain are within the range of 843mg/L and 1566 mg/L. This shows that the drainage system will efficiently remove the extra salts from the soil water profile. The salinity standard deviation within the field ranges between 60 mg/L and 740 mg/L and the coefficient of variation ranges between 0.2 and 1.1 which are higher than the variability of the water table depth.

Relative Crop Yield

Figures 9 and 10 show the first and second moments of crop yield. The within-field crop relative yield ranges between 49.9% and 73.2%. The highest crop yield occurs south of the field despite the relatively high average salinity because of the sub irrigation upward fluxes from the shallow water table. The impact of salinity is not significant because the assumed crop is alfalfa that has $\boldsymbol{\psi_{o50}}$ value of -4300cm. The standard deviation is between 13.5% and 21.6% which correspond to coefficient of variation of 0.22 and 0.31. The highest crop yield variability occurs in the southern part of the field where high salinity and water table standard deviations occurs.

Leaching Fraction

Reclamation of fields with high root zone salinity requires the understanding of the leaching fraction (LF) of applied irrigation. The mean and the standard deviation of leaching fraction values are shown in figures 11 and 12. LF average values range between 15.97% and 50.87% with low values in the southern part of the field. The shallow water table in the southern part seems to be the factor behind low leaching fraction. The standard deviation values of (LF) range between 10.26% and 31.52%. It is noticed that the standard deviation at the southern part is higher than the average, which indicates that negative leaching efficiency is occurring due to the up flux flow in this part of the field.

Drain Hydrograph

Investigating the drainage effluent, in terms of quantity and quality, is important to determine the feasibility of drainage water reuse. In order to achieve this, the 95%, 50% and 5% percentile of drainage flow and salinity hydrograph is plotted figure 13 and 14. The 50% percentile of drainage flow rate fluctuates around 200m^3/day while the 50% percentile of drainage flow salinity fluctuates around 1370 mg/L. The majority of the drained water is the lateral flow from the southern boundary and its salinity is slightly above the lateral flow salinity.

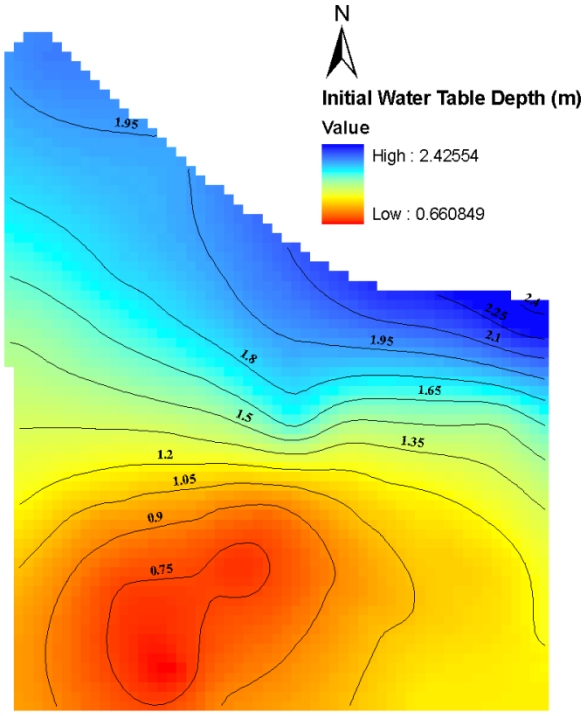

Figure 3. Initial Water Table Depth

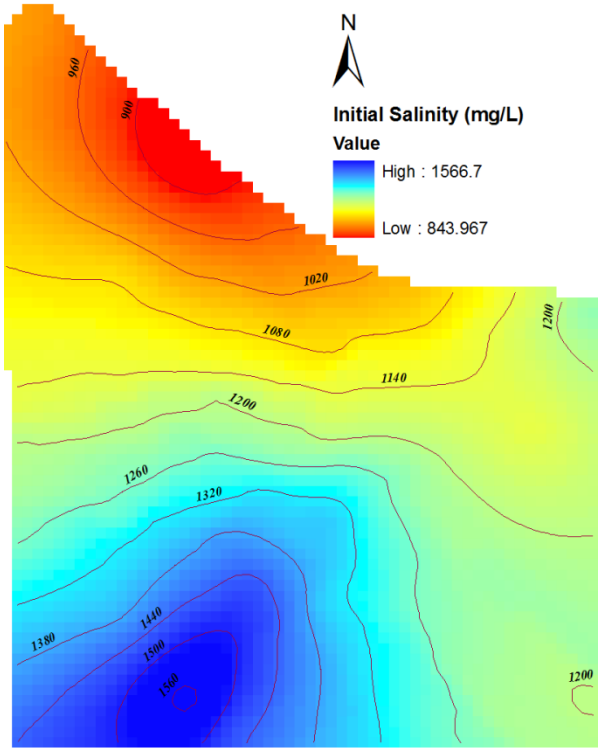

Figure 4. Initial Water Phase Salinity.

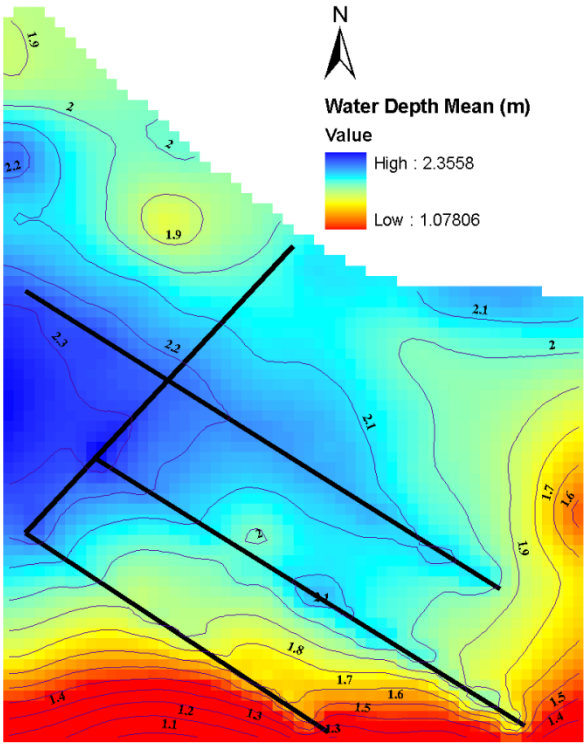

Figure 5. Spatial Average of Groundwater Table Depth at the End of the Season

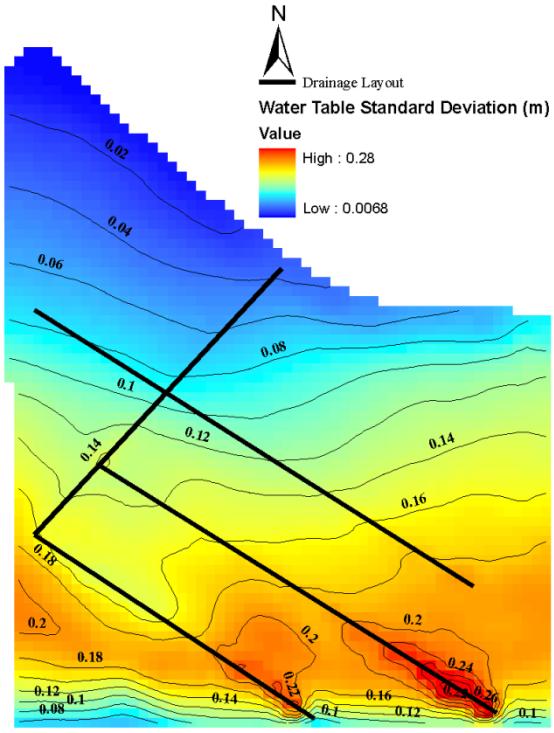

Figure 6. Spatial Standard Deviation of Groundwater Table at the End of the Season

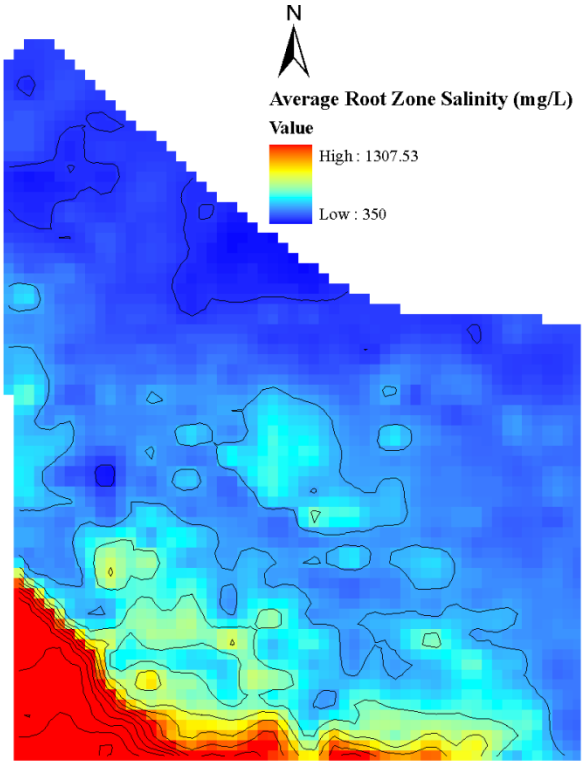

Figure 7. Spatial Average of the Root Zone Average Salinity at the End of the Season

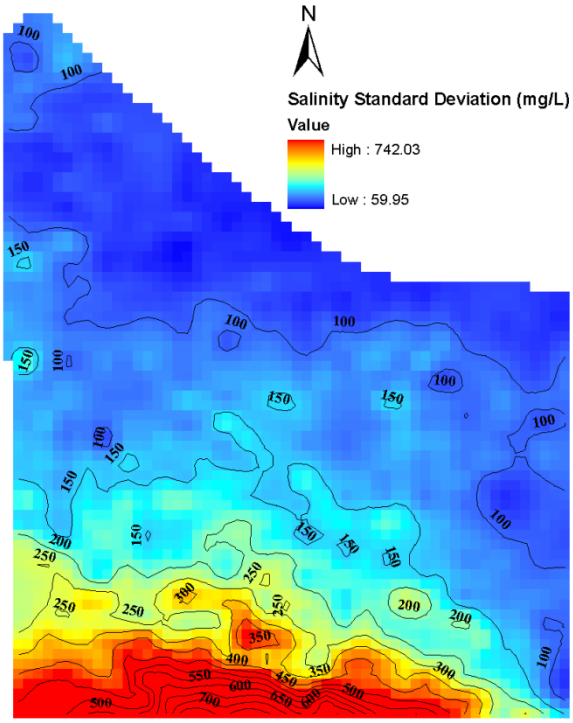

Figure 8. Spatial Standard Deviation of the Root Zone Average Salinity at the End of the Season

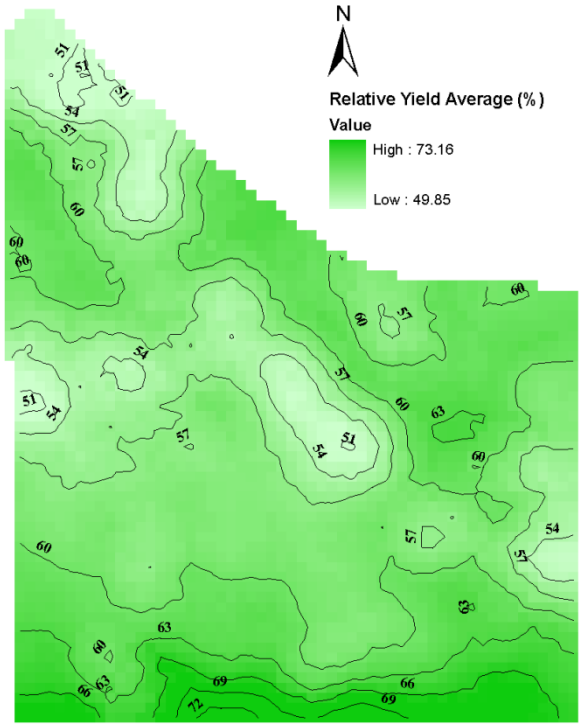

Figure 9. Spatial Average of the Crop Relative Yield

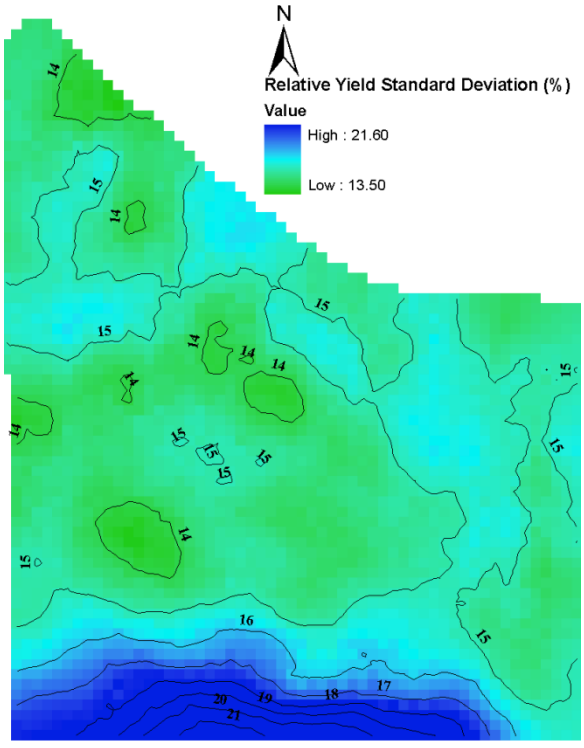

Figure 10. Spatial Standard Deviation of the Crop Relative Yield

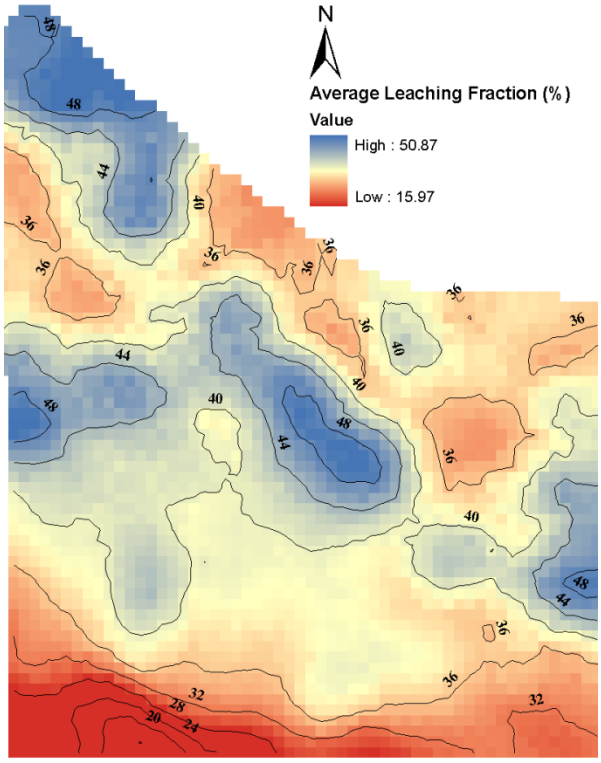

Figure 11. Spatial Average of Salinity Leaching Fraction

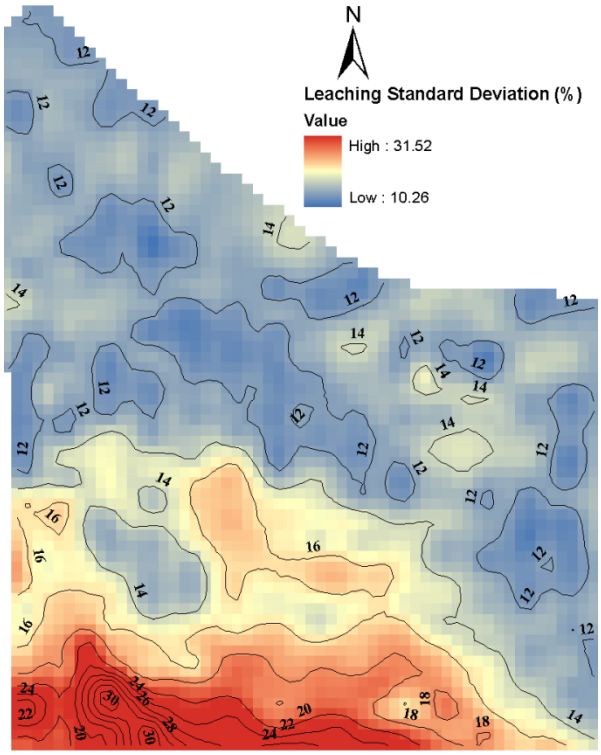

Figure 12. Spatial Standard Deviation of Salinity Leaching Fraction

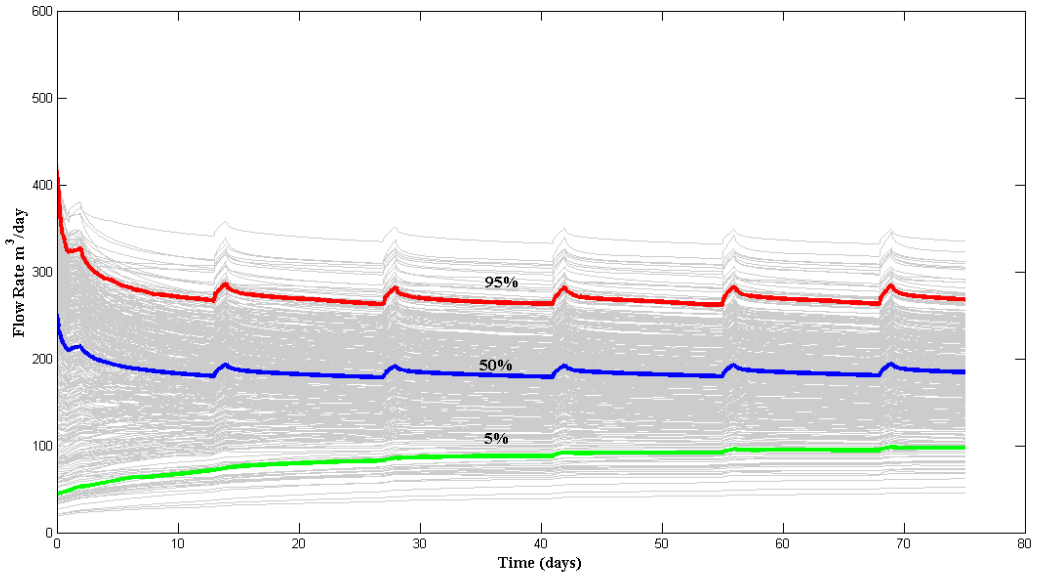

Figure 13. Statistical Percentiles of the Drainage Effluent Hydrograph

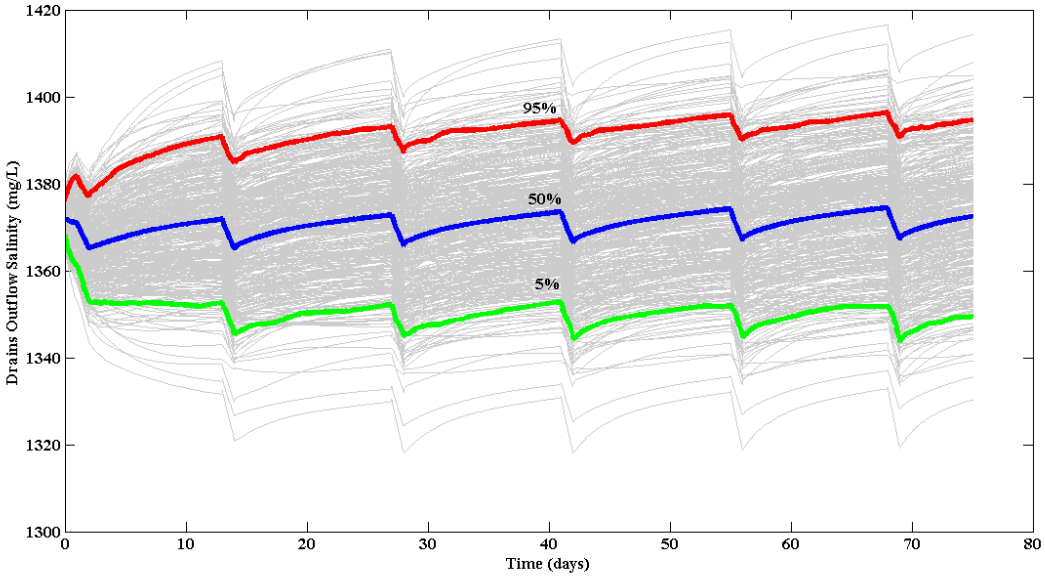

Figure 14. Statistical Percentiles of the Drainage Salinity Hydrograph

8. Conclusion and Summary

The prediction of relative crop yield using numerical models is drastically impacted by the uncertain parameters input. The input parameters are categorized into three group, 1) three-dimensional soil properties, 2) two dimensional parameters such as irrigation uniformity and preferential flow fraction, and finally 3) semi empirical scalar parameters

that control drainage flow, root water uptake and crop yield. The three-dimensional parameters are randomized using the multivariate sequential indicator simulation of the soil-correlated properties. Other parameters are randomized based on field data and published data. The statistical moments of model responses are evaluated spatially such as groundwater depth, crop yield, root zone salinity, and leaching fraction; and temporally such as drainage flow and salinity hydrographs. The results show that significant in-field crop yield variability is evident due to soil variability and water table spatial variability.

Results show that the installation of the subsurface drainage will intercept the saline lateral flow from the southwestern direction and improve the field crop yield. The volume and the quality of drained water are similar to the lateral flow volumes and quality.

References

Alzraiee, A., Garcia, L. and Burnett, R. (2009) "Modeling Spatial and Temporal Variability in Irrigation and Drainage Systems: Improvements to the Colorado State University Irrigation and Drainage Model (CSUID)", Presented and published in the proceedings of the USCID Conference on Irrigation and Drainage for Food, Energy and the Environmental, November 3-6, Salt Lake City, Utah.

Bliesner, Ron D., and Jack Keller. 2001. *Sprinkle and Trickle Irrigation*. The Blackburn Press, March 1.

Bresler, Eshel, and Gedeon Dagan. 1988. Variability of yield of an irrigated crop and its causes: 2. Input data and illustration of results. *Water Resources Research* 24, no. 3: 389. doi:10.1029/WR024i003p00389.

Burkhalter, J. P, T. K Gates, and others. 2005. Agroecological impacts from salinization and waterlogging in an irrigated river valley. *Journal of Irrigation and Drainage Engineering* 131: 197.

Cardon, G. E, and J. Letey. 1992. Plant Water Uptake Terms Evaluated for Soil Water and Solute Movement Models. *Soil Sci. Soc. Am. J.* 56, no. 6: 1876-1880.

Deutsch, Clayton V. 2002. *Geostatistical Reservoir Modeling*. 1st ed. Oxford University Press, USA, April 4.

Deutsch, Clayton V., and André G. Journel. 1997. *GSLIB*. Oxford University Press, January 1.

Deverel, S. J., and J. L Fio. n.d. Groundwater Flow and Solute Movement to Drain Laterals, Western San Joaquin Valley, California 1. Geochemical Assessment. *Water Resources Research* 27, no. 9.

Feddes, Reinder A., Piotr Kowalik, Krystina Kolinska-Malinka, and Henryk Zaradny. 1976. Simulation of field water uptake by plants using a soil water dependent root extraction function. *Journal of Hydrology* 31, no. 1 (September): 13-26. doi:doi: DOI: 10.1016/0022-1694(76)90017-2.

Gates, T. K., L. A. Garcia, and J. W. Labadie. 2006. Toward Optimal Water Management in Colorado's Lower Arkansas River Valley: Monitoring and Modeling to Enhance Agriculture and Environment. *Colorado Water Resources Research Institute Completion Report*, no. 205.

van Genuchten, M. Th. 1980. A Closed-form Equation for Predicting the Hydraulic Conductivity of Unsaturated Soils1. *Soil Science Society of America Journal* 44, no. 5: 892. doi:10.2136/sssaj1980.03615995004400050002x.

Ghassemi, F., A. J. Jakeman, and H. A. Nix. 1995. *Salinisation of Land and Water Resources: Human causes, extent, management and case studies*. CABI, March 2.

Goswami, Debashish, and Prasanta K. Kalita. 2009. Simulation of base-flow and tile-flow for storm events in a subsurface drained watershed. *Biosystems Engineering* 102, no. 2 (February): 227-235. doi:doi: DOI: 10.1016/j.biosystemseng.2008.11.004.

Haan, P. K., and R. W. Skaggs. 2003. Effect of parameter uncertainty on DRAINMOD predictions: I. Hydrology and yield. *Transactions of the ASAE* 46, no. 4: 1061–1067.

Harbaugh, A. W, E. R Banta, M. C Hill, and M. G McDonald. 2000. *MODFLOW-2000, The U. S. Geological Survey Modular Ground-Water Model-User Guide to Modularization Concepts and the Ground-Water Flow Process*. United States Geological Survey.

Hoffman, Glenn J., Robert G. Evans, Marvin Eli Jensen, Derrel L. Martin, and Ronald L. Elliott. 2007. *Design And Operation Of Farm Irrigation Systems*. 2nd ed. American Society of Agricultural & Biological, October 30.

Hopmans, J. W, and K. L Bristow. 2002. Current capabilities and future needs of root water and nutrient uptake modeling. *Advances in Agronomy* 77: 103–183.

Houk, Eric, W. Marshall Frasier, and Eric Schuck. 2004. *The Regional Effects Of Waterlogging And Soil*

Salinization On A Rural County In The Arkansas River Basin Of Colorado. Western Agricultural Economics Association. http://ideas.repec.org/p/ags/waeaho/36229.html.

Johnson, Norman L., Samuel Kotz, and N. Balakrishnan. 1995. *Continuous Univariate Distributions, Vol. 2*. 2nd ed. Wiley-Interscience, May 8.

Journel, A. 1999. Markov Models for Cross-Covariances. *Mathematical Geology* 31, no. 8 (November 1): 955-964.

Konikow, Leonard F., and John D. Bredehoeft. 1992. Ground-water models cannot be validated. *Advances in Water Resources* 15, no. 1: 75-83. doi:doi: DOI: 10.1016/0309-1708(92)90033-X.

Miles, D. L. 1977. Salinity in the Arkansas Valley of Colorado."Interagency Agreement Report EPA-IAG-D4-0544. *Environmental Protection Agency, Denver, Colorado*.

Molz, Fred J. 1981. Models of water transport in the soil-plant system: A review. *Water Resour. Res.* 17, no. 5: 1245-1260.

Montazar, Aliasghar. 2010. Predicting alfalfa hay production as related to water distribution functions. *Irrigation and Drainage* 59, no. 2: 189-202.

Muralidharan, Daya, and Keith C. Knapp. 2009. Spatial dynamics of water management in irrigated agriculture. *Water Resources Research* 45, no. 5 (5). doi:10.1029/2007WR006756. http://www.agu.org/pubs/crossref/2009/2007WR006756.shtml.

Oreskes, Naomi, Kristin Shrader-Frechette, and Kenneth Belitz. 1994. Verification, Validation, and Confirmation of Numerical Models in the Earth Sciences. *Science* 263, no. 5147. New Series (February 4): 641-646.

Postel, Sandra. 1989. *Water for agriculture : facing the limits*. Washington D.C.: Worldwatch Institute.

Rhoades, J. D., A. Kandiah, and A. M. Mashali. 1992. The use of saline waters for crop production. *FAO Irrigation and Drainage Paper (FAO)* 48.

Rubin, Yoram, and Dani Or. 1993. Stochastic modeling of unsaturated flow in heterogeneous soils with water uptake by plant roots: The Parallel Columns Model. *Water Resources Research* 29, no. 3: 619. doi:10.1029/92WR02292.

Schaap, M. G, F. J Leij, and M. T van Genuchten. 2001. Rosetta: A computer program for estimating soil hydraulic parameters with hierarchical pedotransfer functions. *Journal of Hydrology* 251, no. 3: 163–176.

Schnepf, R. 2010. Agriculture-Based Biofuels: Overview and Emerging Issues.

Shalhevet, J., A. Vinten, and A. Meiri. 1986. Irrigation interval as a factor in sweet corn response to salinity. *Agronomy journal (USA)*.

Steenhuis, T. S, J. Boll, G. Shalit, J. S Selker, and I. A Merwin. 1994. A simple equation for predicting preferential flow solute concentrations. *J. Environ. Qual* 23, no. 5: 1058–1064.

Tanji, Kenneth K. 1990. *Agricultural Salinity Assessment and Management*. Amer Society of Civil Engineers, August.

Umali, Dina L., and Dina Umali-Deininger. 1993. *Irrigation-induced salinity: a growing problem for development and the environment*. World Bank Publications, November.

Van Genuchten, M. T, and US Salinity Laboratory. 1987. *A numerical model for water and solute movement in and below the root zone*. United States Department of Agriculture Agricultural Research Service US Salinity Laboratory.

Veenhof, D. W., and R. A. McBride. 1994. A preliminary performance evaluation of a soil water balance model (SWATRE) on corn producing croplands in the RM of Haldimand-Norfolk. *Soil compaction susceptibility and compaction risk assessment for corn production. Centre for Land and Biological Resources Research AAFC, Ottawa*: 112–142.

Wackernagel, Hans. 2003. *Multivariate Geostatistics*. 3rd ed. Springer, April 10.

Wang, X., J. R. Frankenberger, and E. J. Kladivko. 2006. Uncertainties in DRAINMOD predictions of subsurface drain flow for an Indiana silt loam using the GLUE methodology. *Hydrological Processes* 20, no. 14: 3069-3084.

Warrick, A. W., and W. R. Gardner. 1983. Crop yield as affected by spatial variations of soil and irrigation. *Water Resources Research* 19, no. 1: 181. doi:10.1029/WR019i001p00181.

Wichelns, Dennis. 1999. An economic model of waterlogging and salinization in arid regions. *Ecological Economics* 30, no. 3 (September): 475-491. doi:doi: DOI: 10.1016/S0921-8009(99)00033-6.

Xu, Moujin, and Yoram Eckstein. 1997. Statistical Analysis of the Relationships Between Dispersivity and Other Physical Properties of Porous Media. *Hydrogeology Journal* 5, no. 4 (April 1): 4-20.